Journal of Environmental Radioactivity 100 (2009) 375–395

Contents lists available at ScienceDirect

Journal of Environmental Radioactivity

journal homepage: www.elsevier.com/locate/jenvrad

Sources and pathways of ^{90}Sr in the North Atlantic–Arctic region: present day and global warming

Yongqi Gao [a,b,c,*], Helge Drange [b,c,d], Ola M. Johannessen [a,d], Lasse H. Pettersson [a]

[a] Nansen Environmental and Remote Sensing Center, Bergen, Norway
[b] Nansen-Zhu International Research Center, Beijing, China
[c] Bjerknes Center for Climate Research, Bergen, Norway
[d] Geophysical Institute, University of Bergen, Norway

ARTICLE INFO

Article history:
Received 31 March 2008
Received in revised form
30 December 2008
Accepted 11 January 2009

Keywords:
^{90}Sr
Sources
Pathways
Global warming

ABSTRACT

The spatial and temporal distributions of the anthropogenic radionuclides ^{137}Cs and ^{90}Sr, originating from nuclear bomb testing, the Sellafield reprocessing plant in the Irish Sea (UK), and from the Ob and Yenisey river discharges to the Arctic Ocean, have been simulated using the global version of the Miami Isopycnic Coordinate Ocean Model (MICOM). The physical model is forced with daily atmospheric re-analysis fields for the period of 1948–1999. Comparison of the temporal evolution of the observed and the simulated concentrations of ^{90}Sr has been performed in the Kara Sea. The relative contributions of the different sources on the temporal and spatial distributions of the surface ^{90}Sr are quantified over the simulated period. It follows that the Ob river discharge dominated the surface ^{90}Sr over most of the Arctic Ocean and along the eastern and western coasts of Greenland before 1960. During the period of 1980–1990, the atmospheric fallout and the Ob river discharge were equally important for the ^{90}Sr distribution in the Arctic Ocean. Furthermore, an attempt has been made to explore the possible dispersion of accidental released ^{90}Sr from the Ob and Yenisey rivers under a global warming scenario ($2 \times CO_2$). The difference between the present-day and the global warming scenario runs indicates that more of the released ^{90}Sr from the Ob and Yenisey rivers is confined to the Arctic Ocean in the global warming run, particularly in the near coastal, non-European part of the Arctic Ocean.

1. Introduction

Radioactive contamination of the Arctic environment has received much attention over the last decades. This is caused by the fact that there are many actual and potential radioactive sources within and near the Arctic region, and that the Arctic food chains are particularly vulnerable to radioactive exposure.

Accurate quantification of the temporal–spatial distributions of the radionuclides can be achieved by combining precise source functions of the radionuclides, available *in situ* observations, and 3-dimensional simulation by Ocean General Circulation Models (OGCMs). The main focus of this paper is on the latter.

It has been demonstrated that the OGCMs can be a powerful tool to simulate the temporal and spatial distributions of man-made radionuclides (e.g. Nies et al., 1998; Gerland et al., 2003; Tsumune et al., 2003; Karcher et al., 2004; Gao et al., 2004, 2005; Orre et al., 2007). For instance, Tsumune et al. (2003) performed a global simulation of ^{137}Cs and ^{239,240}Pu with the source from the atmospheric fallout, and Gerland et al. (2003) performed a simulation of ^{99}Tc with the source from the Sellafield reprocessing plant using a regional OGCM. More recently, Gao et al. (2004) used a global version of the MICOM (Nansen Environmental and Remote Sensing Center version of MICOM; Bleck et al., 1992) to examine the transport of the radionuclides ^{90}Sr and ^{137}Cs from the atmospheric fallout and the Sellafield discharge in the Atlantic–Arctic Oceans. The latter study showed that the simulated temporal evolutions of surface ^{137}Cs are in fairly good agreement with the observations to east of Scotland, west of Norway and in the Barents Sea, and the transit time for the radionuclides released from the Sellafield to the Barents Sea is about 4–5 years, in accordance with the observations by Kershaw and Baxter (1995). It was also shown that in the Atlantic waters off the coast of Norway and in the southern Barents Sea, the atmospheric fallout of ^{90}Sr and ^{137}Cs dominated over the Sellafield release up to the mid1960s and after the early 1990s, whereas Sellafield release was the main source for the two radionuclides in the 1970s and 1980s.

* Corresponding author at: Nansen Environmental and Remote Sensing Center, Thormoehlemsgate 47, 5006 Bergen, Norway. Tel.: +47 55205800; fax: +47 55205801.
E-mail address: yongqi.gao@nersc.no (Y. Gao).

0265-931X/$ – see front matter © 2009 Elsevier Ltd. All rights reserved.
doi:10.1016/j.jenvrad.2009.01.003

In the present study, the same global version of MICOM as in Gao et al. (2004) is used to examine the spreading and the concentrations of man-made ^{90}Sr originating from nuclear bomb testing, the Sellafield release in the Irish Sea, and transport from the Ob and Yenisey rivers to the Arctic Ocean. The relative contributions of the different sources on the spatial-temporal distributions of the surface ^{90}Sr over the period of 1948–1999 are assessed. It should be mentioned that the Chernobyl accidental release in 1986 is not included in this study.

Furthermore, ocean circulation and mixing processes govern the transport of all conservative substances in the ocean. Since the global climate system changes as a result of increasing greenhouse gases in the atmosphere, the dynamics and the thermodynamics of the ocean will also change. The changed ocean climate will have consequences for the transport and mixing of radionuclides in the Atlantic–Arctic region. To assess the spreading and mixing characteristics of accidentally released radionuclides under a global warming scenario, in addition to the above-mentioned hind-cast simulation, twin experiments with the OGCM have been performed with present day forcing and with possible forcing resembling the future climate in the 21st century. The differences in the transport and mixing between the two climate situations provide a scenario for possible changes in the transport routes and concentration distributions of radionuclides.

The OGCM used in this work has been tested against observed quantities in the region of interest (Nilsen et al., 2003; Gao et al., 2003, 2004, 2005; Drange et al., 2005; Eldevik et al., 2005; Hatun et al., 2005; Orre et al., 2007). In general, the model is able to reproduce the ocean circulation and thermodynamics in a fairly realistic way. It is therefore believed that the model system is an useful and appropriate tool to simulate the advective transport and dispersive mixing of radionuclides which behave conservatively in sea water.

The paper is organized as follows: A description of the model system is provided in Section 2. The radionuclides simulation is described in Section 3. In Section 4, a brief overview of the ocean circulation in the Atlantic–Arctic Ocean is given, together with the observation-derived pathway of the Sellafield discharge. The obtained results from the hind-cast and the future simulations are given in Sections 5 and 6, respectively, and finally the paper is summarized in Section 7.

2. Model description and configuration

The model system applied in this study has been used in Gao et al. (2004) (hereafter G04). Some of the key features are repeated here:

The model has 23 layers with fixed potential densities, and an uppermost mixed layer (ML) with temporal and spatial varying density. In the horizontal, the model is configured with a local orthogonal grid mesh with one pole over North America and one pole over western part of Asia (Bentsen et al., 1999), yielding a grid-spacing of about 90–120 km in the North Atlantic–Arctic region.

The model was initialized by the January Levitus and Boyer (1994) and Levitus et al. (1994) climatological temperature and salinity fields, respectively, a 2 m thick sea-ice cover based on climatological sea-ice extent, and an ocean at rest. The model was first spin-up for 180 years with monthly-mean atmospheric forcing fields derived from the NCEP/NCAR re-analysis (Kalnay et al., 1996), and was then continued with daily NCEP/NCAR forcing, repeating the period 1974–1978 twice. The period 1974–1978 was chosen because of the relatively neutral North Atlantic Oscillation (NAO; Hurrell, 1995) conditions of these years. Thereafter, for the hind-cast simulation, the model was integrated with daily forcing for the period 1948–1999.

For the simulation of ^{90}Sr originating from accidental releases in the Ob and Yenisey rivers, twin-integrations have been conducted. The base-line integration is similar to the hind-cast simulation described above, i.e., a simulation under present climate conditions covering the time period from 1970 to 2000 with the daily NCEP/NCAR forcing. For the global warming scenario, daily atmospheric forcing fields were extracted from a $2 \times CO_2$ simulation performed with the Bergen Climate Model (BCM; Furevik et al., 2003; Sorteberg et al., 2005). To ensure that the OGCM is driven by forcing fields consistent with the NCAR/NCEP forcing, the following procedure was adopted: In step one, the mean daily values of all of the atmospheric forcing fields from the last 30 years of the $2 \times CO_2$ simulation were stored, and then the difference between these daily forcing fields and the climatological mean of the same fields from a control integration with BCM was computed. In this way, the obtained product is the daily change in the atmospheric forcing fields caused by increased concentration of atmospheric CO_2 in BCM. Finally, the daily forcing anomalies from the $2 \times CO_2$ BCM simulation were added to the mean of the NCAR/NCEP re-analysis fields for the period 1970–2000. For the $2 \times CO_2$ forcing, the integration has been performed twice with the same forcing to stabilize the simulated surface water.

3. Setup of the radionuclides simulation

3.1. The hind-cast simulation

The important sources of the radionuclides in the North Atlantic–Arctic region are the nuclear bomb testing, the Chernobyl accident and releases from the European reprocessing plants Sellafield (UK) and Cap de La Hague (France) (Nies et al., 1998; Strand et al., 2002). The Sellafield discharge has been dominant over that of Cap de La Hague in terms of quantities and impact for the majority of the northern waters (Kershaw and Baxter, 1995). Therefore, the dispersion of the radionuclides released from Cap de La Hague is not considered in this study. The time evolutions of ^{137}Cs and ^{90}Sr from the Sellafield release and from the nuclear bomb testing were provided by S. Nielsen (personal communication, 2001; see also Fig. 3 in G04). The atmospheric fallout provides the present background concentration of the surface and sub-surface waters in the region, while the Sellafield discharge is one of the major sources of radioactive contamination in the Arctic Ocean since the 1970s (Strand et al., 1996).

Furthermore, radioactive contaminations have been discharged from Russian nuclear facilities at the high northern latitudes. Generally speaking, those discharges played less important roles in the overall radioactive contamination. However, Russian nuclear facilities that discharge into the Ob and Yenisey river systems and eventually reach the Arctic Ocean need to be considered since their discharges have been high historically (Strand et al., 1998). There is concern about whether and how they have contaminated the Arctic Ocean, and whether and how potential accidents can lead to further contamination. To have the input flux of ^{90}Sr transported from the Ob and Yenisey rivers, the 1D river model (Zheleznyak et al., 1992) and the 3D estuary model (Margvelashvili et al., 1997) were used with the output from 1D river model as the input of the 3D estuary model. Both the 1D river model and the 3D estuary model have been validated against the available observations. Finally, the simulated temporal distribution of the ^{90}Sr concentration by the 3D estuary model is used as the source function for the results presented here. Fig. 1 shows reconstructed time evolutions of ^{90}Sr caused by the river discharges at the mouths of the Ob and Yenisey rivers in the Kara Sea for the past 50 years (Johannessen et al., 2003).

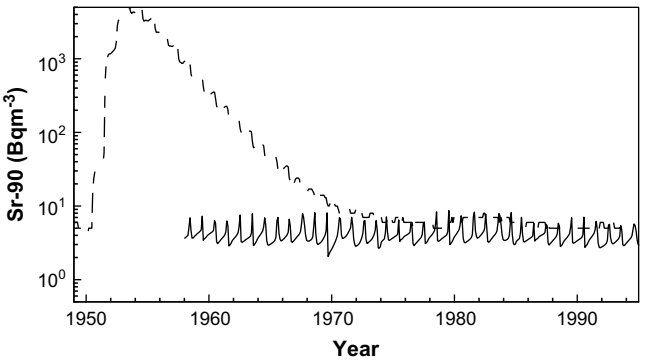

Fig. 1. The temporal evolution of ^{90}Sr concentration (Bq m^{-3}) at the mouth of Yenisey (solid line) and Ob rivers (dashed line) in the Kara Sea caused by the river discharge (monthly data from 1949 to 1993 for Ob river and from 1958 to 1995 for Yenisey river). Data from Johannessen et al. (2003).

Four tracers in the hind-cast simulation will be discussed later on: the atmospheric fallout induced ^{90}Sr, the Sellafield discharge induced ^{90}Sr and the ^{90}Sr caused by the discharges from the Ob and Yenisey rivers. The simulated dispersion of ^{137}Cs caused by the atmospheric fallout and the Sellafield discharge will be discussed briefly since it is identical with that of G04. The initial fields of all the radionuclides are set to zero and the integration starts from 1948 and ends in 1999.

3.2. Simulation on accidental releases

The hypothetical accidents were assumed for the simulation on accidental releases. In the Ob river, the scenario assumes a sudden and uncontrollable break-down of the dam of the reservior-11 at Mayak. In the Yenisey river, the hypothetical accident at Mining Combine (MCC) assumes an instantaneous release of ^{90}Sr. The river model is used to generate the time evolution of ^{90}Sr concentration at the Ob bay and at the Yenisey Gulf of the Kara Sea. Fig. 2 shows the proposed accidental daily release of ^{90}Sr from the Ob and Yenisey rivers. The maximum accidental releases take place in summer with the peak values of 116 Bq m^{-3} for the Ob river and 302 Bq m^{-3} for the Yenisey river. The integration for the accidental release scenario under present-day climate condition starts from 1970 with zero concentrations in the sea water and ends in 2000, whereas the integration under global warming scenario starts from 2050 with zero concentrations in the sea water and ends at 2080.

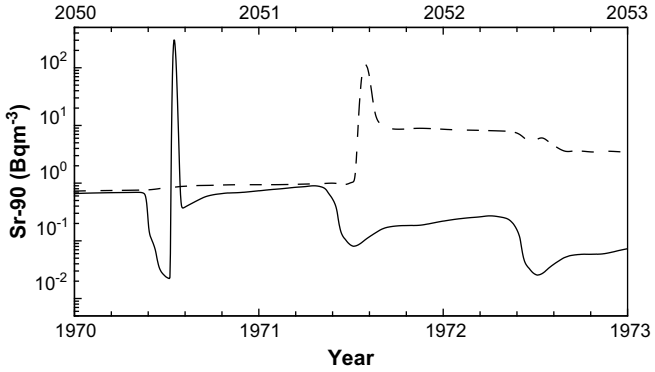

Fig. 2. Proposed accidental release of ^{90}Sr (Bq m^{-3}) from the Ob river (dashed line) and the Yenisey river (solid line) (Johannessen et al., 2003). The *x*-axes indicate the time for the simulation with the present day (lower *x*-axis) and the $2 \times CO_2$ (upper *x*-axis) climate forcing.

4. Ocean circulation and radionuclides

The ocean circulation in the North Atlantic–Arctic region is mainly governed by the northward-flowing warm and saline Atlantic Water (AW) and the southward-flowing cold and fresh Polar Water (PW). The AW enters the Greenland–Iceland–Norwegian Seas (Nordic Seas) mainly over the ridges between Iceland and Scotland (Hansen and Østerhus, 2000), and continues northward along the Norwegian coast as the Norwegian Atlantic Current (NAC). One branch of the AW enters the Barents Sea (2.3 Sv, 1 Sv = 10^6 m^3 s^{-1}; Ingvaldsen et al., 2002), and the other flows towards the Fram Strait as the West Spitsbergen Current (WSC). A part of the AW carried with WSC flows into the Arctic Ocean, whereas the rest recirculates and flows southward. In the Arctic Ocean, the surface ocean circulation is characterized by the Beaufort Gyre and the Transpolar Drift (TPD). The PW leaves the Arctic with the East Greenland Current (EGC) on the western side of the Fram Strait, continuing southward along the coast of Greenland. Most of PW flows through the Denmark Strait and enters the subpolar gyre.

The mean simulated surface current in the Atlantic–Arctic region is, in general, in accordance with observations (G04).

Summarized by Kershaw and Baxter (1995), the pathway of the soluble radionuclides ^{137}Cs and ^{90}Sr from Sellafield to the Arctic follows: Initially the tracer is carried northward from the Irish Sea through the North Channel, and then flows along the coast of Scotland into the North Sea. The tracer is transported northward before branching off northern Norway: One branch passes eastwards into the Barents Sea; the other passes through the Fram Strait with the WSC. The simulated pathway of radionuclides ^{137}Cs from Sellafield discharge to the Arctic is in fairly good agreement with the observation (G04).

5. Results from the hind-cast simulation

Figs. 3–8 show the simulated spatial and temporal distributions of surface ^{90}Sr concentrations and the relative contributions from the atmospheric fallout, the Sellafield release and the Ob river discharge from 1955 to 1999, respectively.

High concentrations of ^{90}Sr with values between several hundreds to three thousands of Bq m^{-3} were found in the area close to the mouth of the Ob river in the Kara Sea in 1955. Concentrations below 5 Bq m^{-3} were found on the eastern and western sides of the North Atlantic and in the coastal waters off western Norway (Fig. 3a). The atmospheric fallout dominated the ^{90}Sr distribution in the North Atlantic and in the coastal waters off western Norway (Fig. 3b), whereas the Ob river discharge dominated the ^{90}Sr distribution in the Arctic Ocean and the western side of the Nordic Seas (Fig. 3d). The Sellafield discharge mainly influenced the North Sea (Fig. 3c). From 1955 to 1960, the radioactivity increased in the central Arctic Ocean, the North Atlantic and the Nordic Seas (Fig. 4a). The increased activity in the eastern North Atlantic and the eastern Nordic Seas was mainly caused by the atmospheric fallout (Fig. 4b), whereas the Ob river discharge was responsible for the increased activity in the central Arctic Ocean and in the coastal waters of the south-eastern Greenland (Fig. 4d). Furthermore, a fraction of the ^{90}Sr that was transported by the EGC could also be found north of Iceland. Note that the Sellafield signal had branched into two parts with one entering the Barents Sea and the other heading towards the Fram Strait (Fig. 4c). In early 1970s, the relatively high radioactivity could be found from the northern Kara Sea to the Fram Strait (Fig. 5a). The atmospheric fallout was the main contributor to the ^{90}Sr distribution in the North Atlantic, in the eastern Nordic Seas, and to a less extent, in the western Nordic Seas (Fig. 5b), whereas the Ob

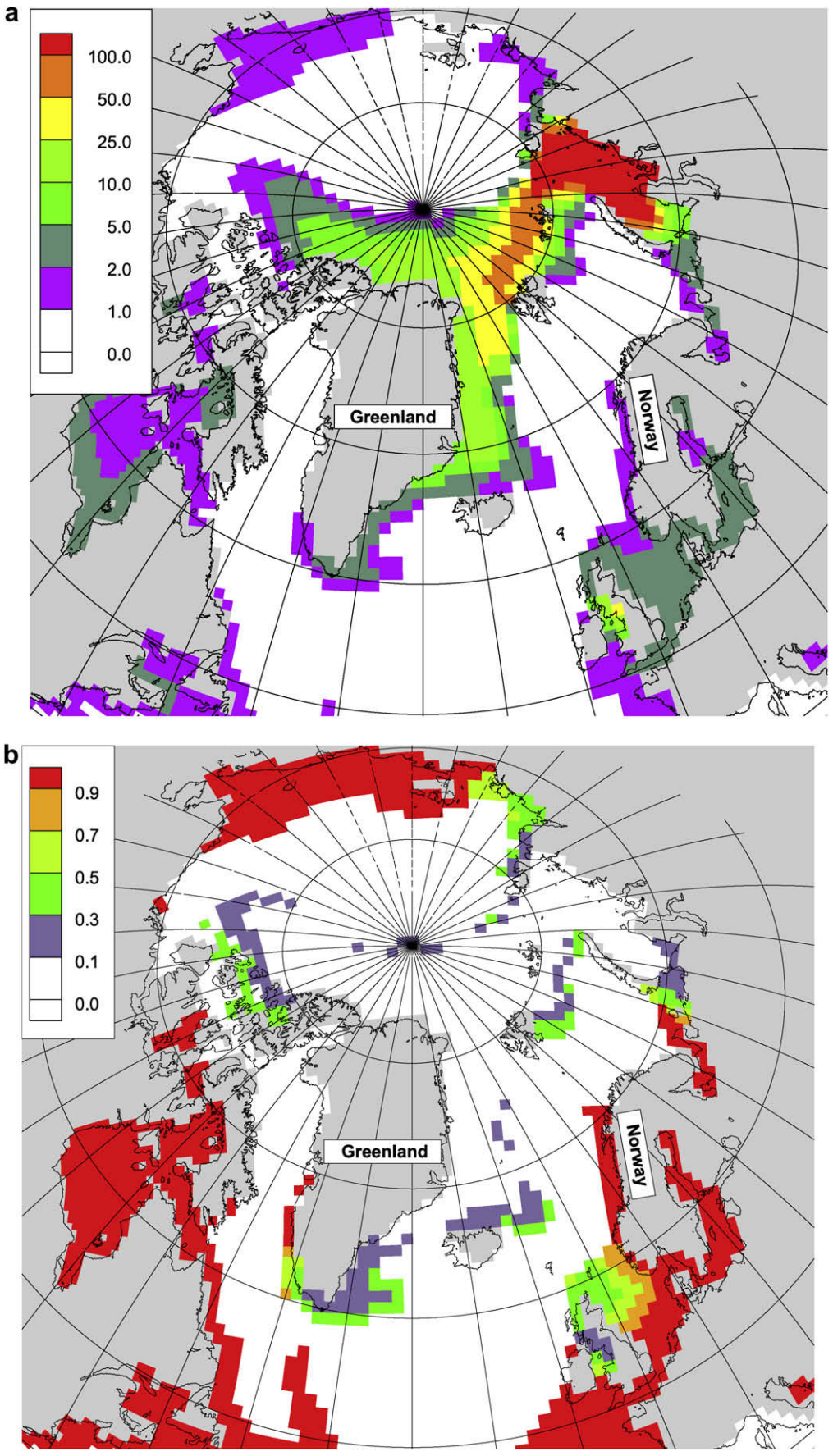

Fig. 3. Simulated total surface concentration of ^{90}Sr (Bq m^{-3}) in 1955 (a), the ratio of atmospheric fallout induced ^{90}Sr to total ^{90}Sr (b), the ratio of Sellafield release induced ^{90}Sr to total ^{90}Sr (c) and the ratio of Ob river discharge induced ^{90}Sr to total ^{90}Sr (d). The cut off value of the ^{90}Sr concentration is 1 Bq m^{-3}.

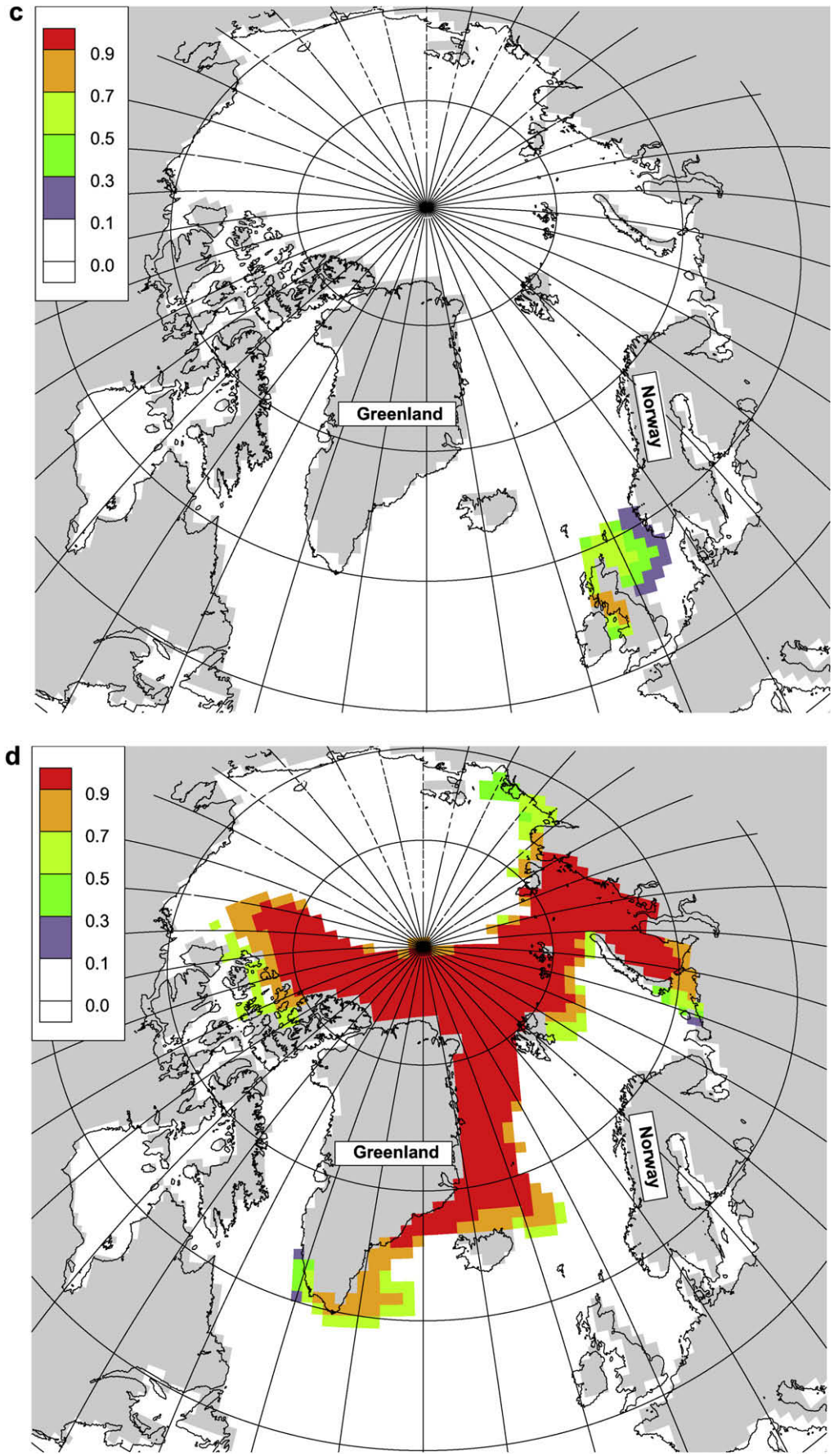

Fig. 3. (*continued*).

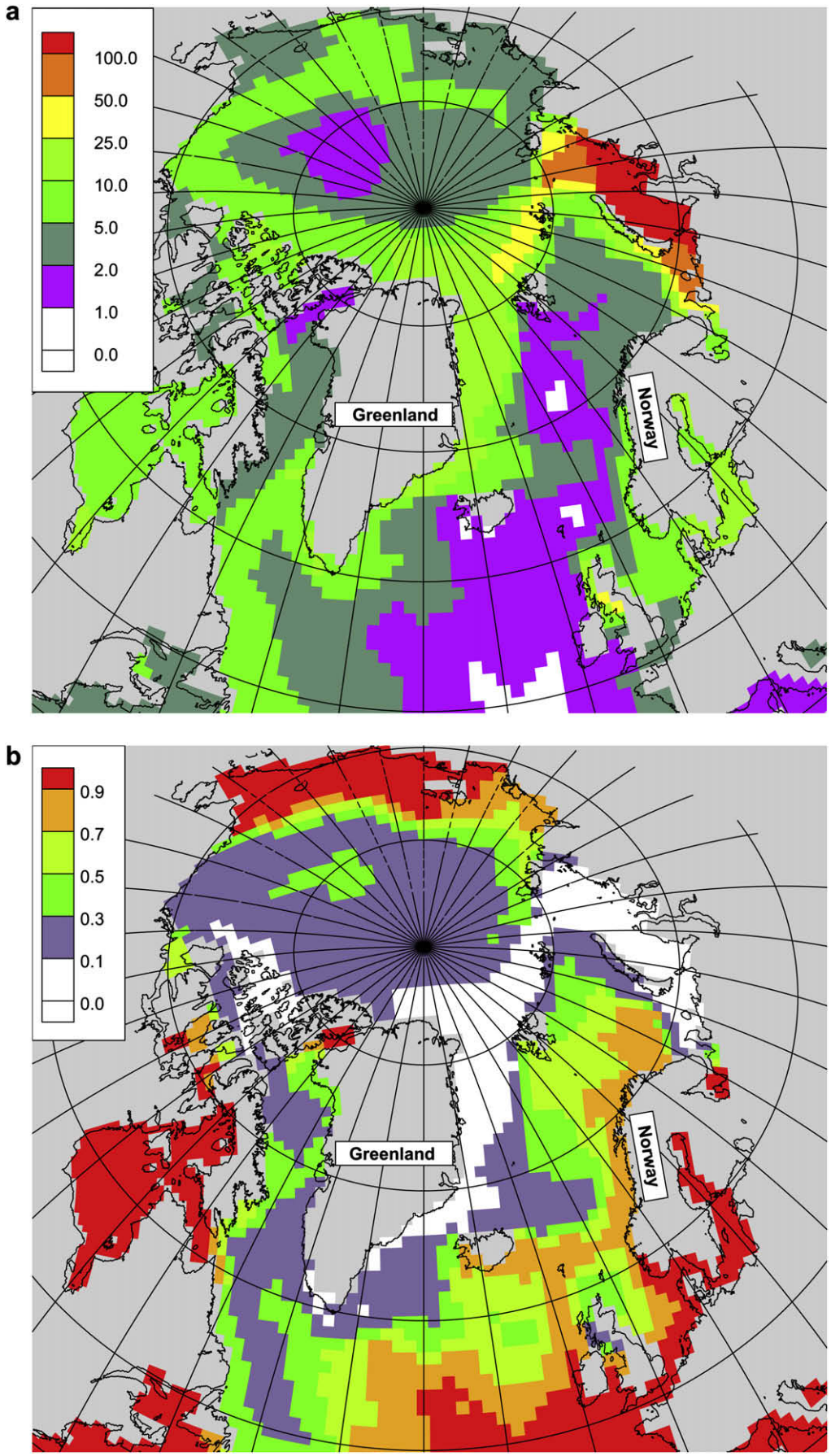

Fig. 4. As Fig. 3, but for year 1960.

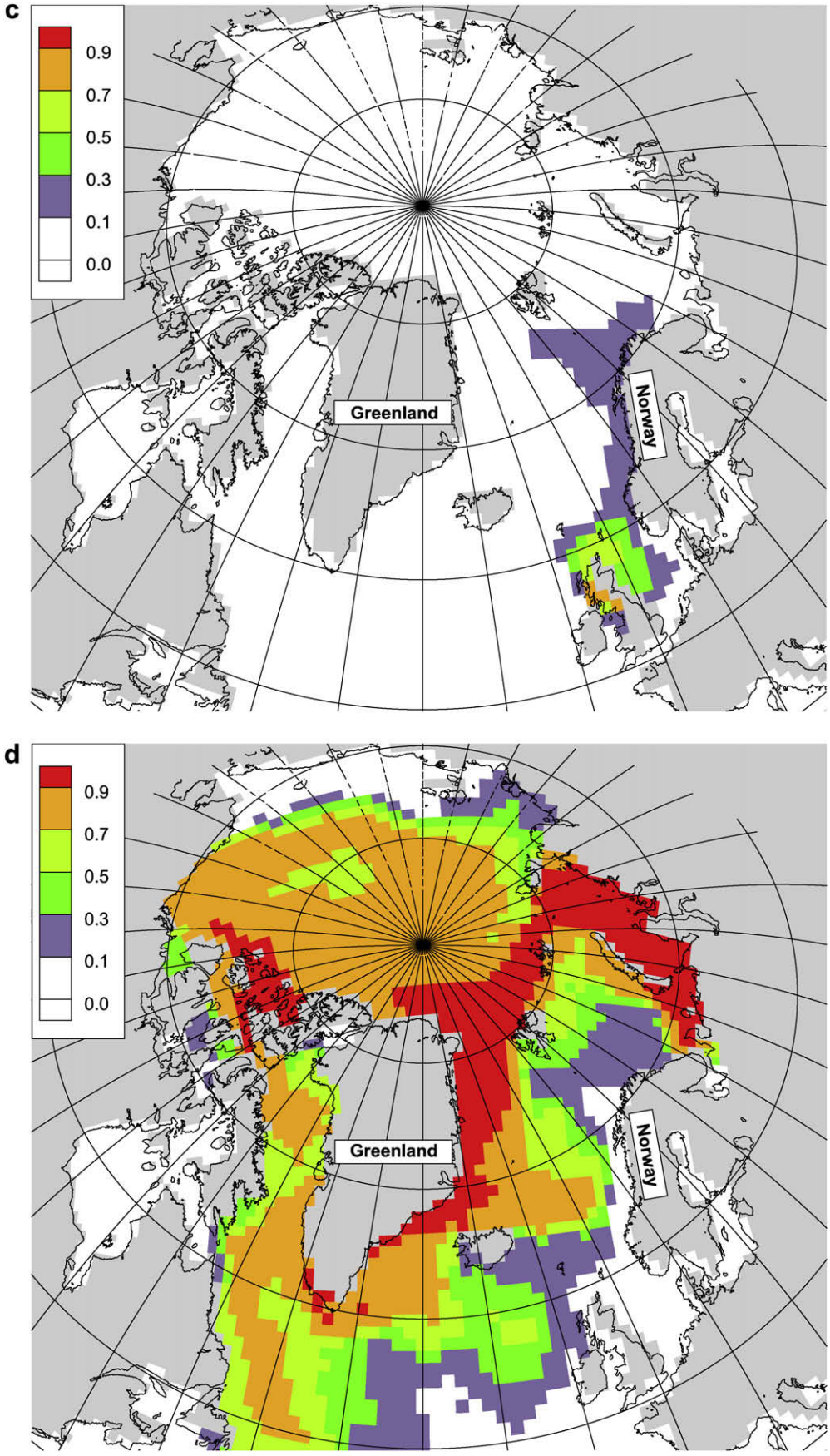

Fig. 4. (*continued*).

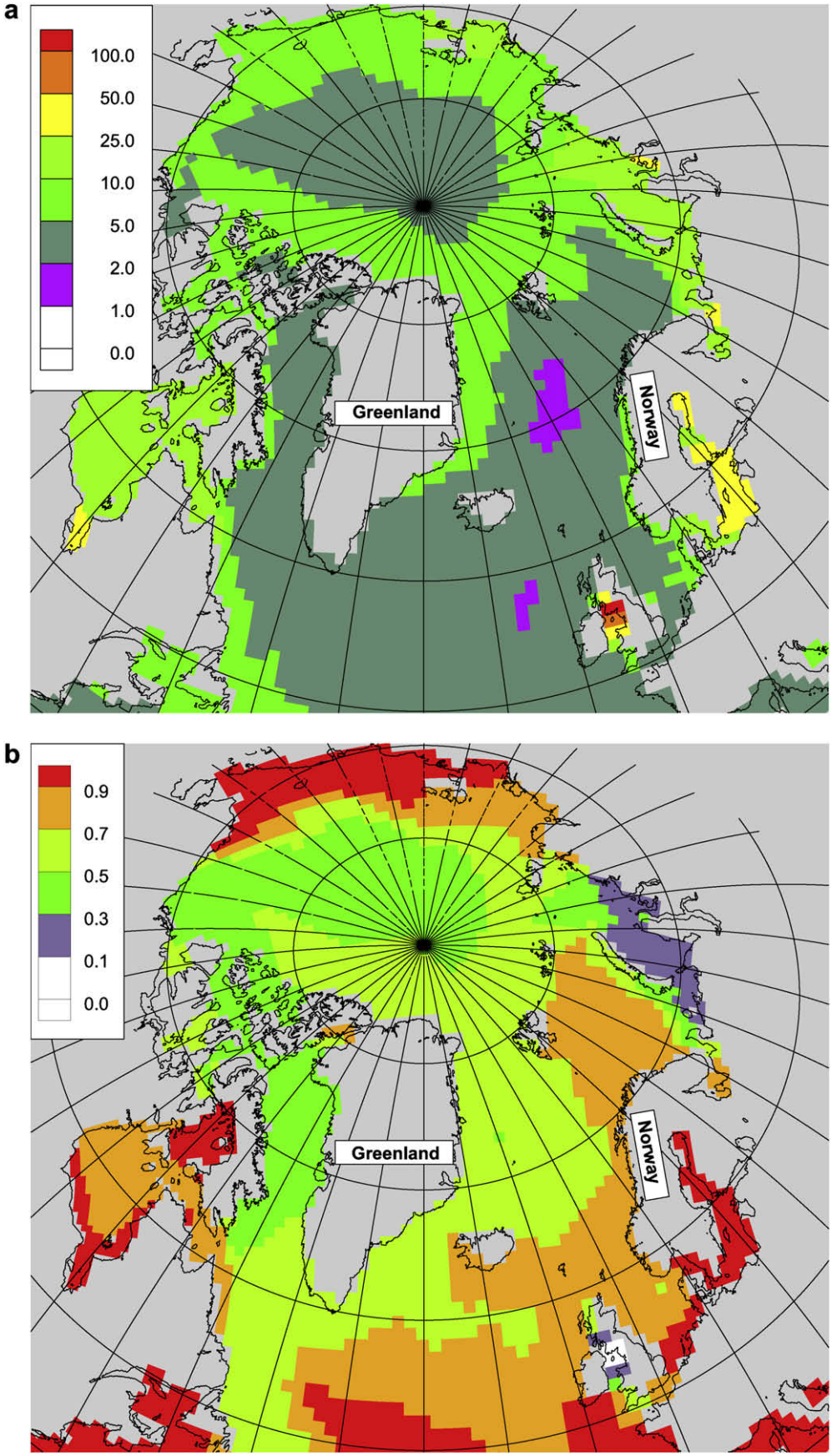

Fig. 5. As Fig. 3, but for year 1970.

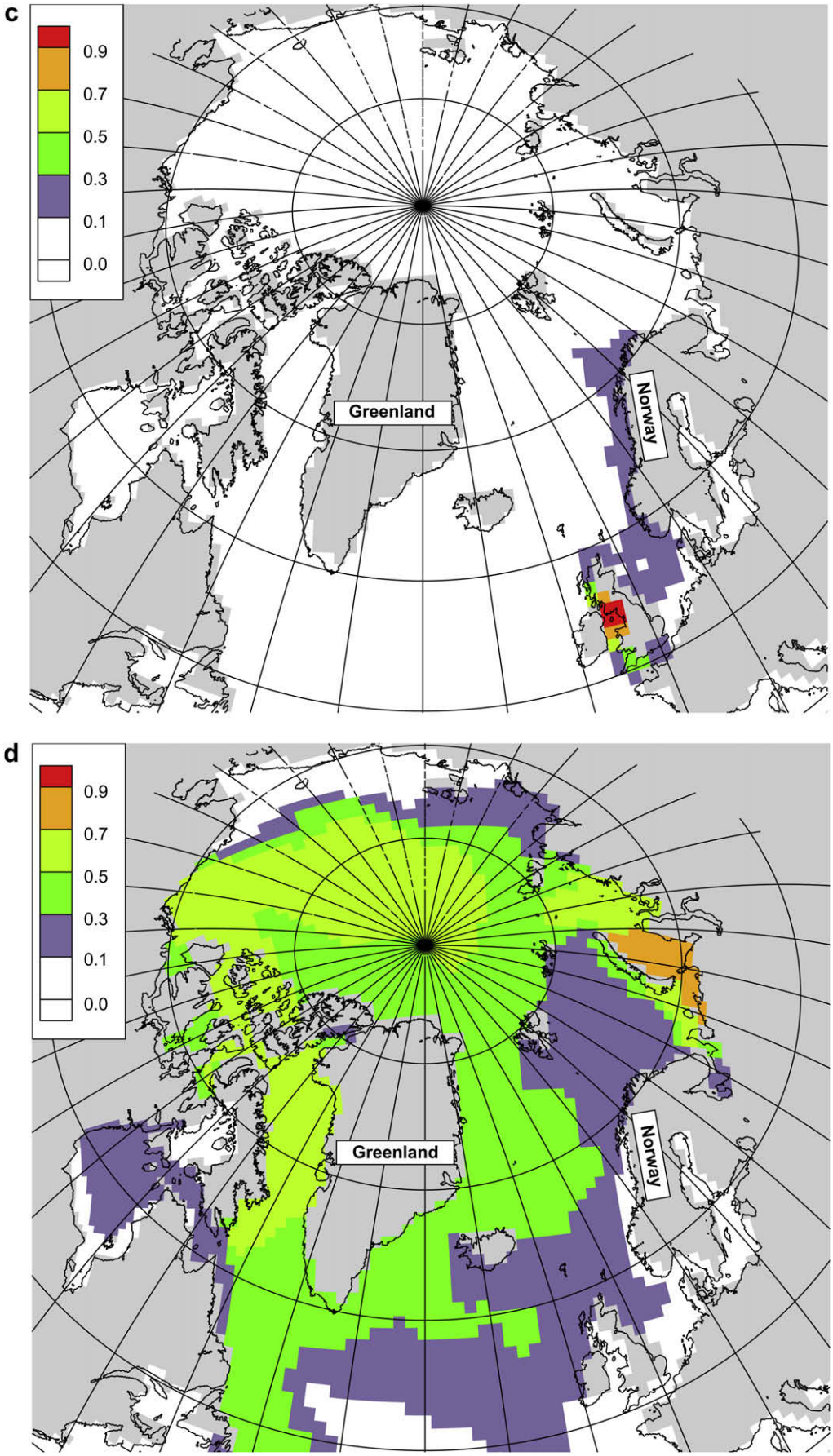

Fig. 5. (*continued*).

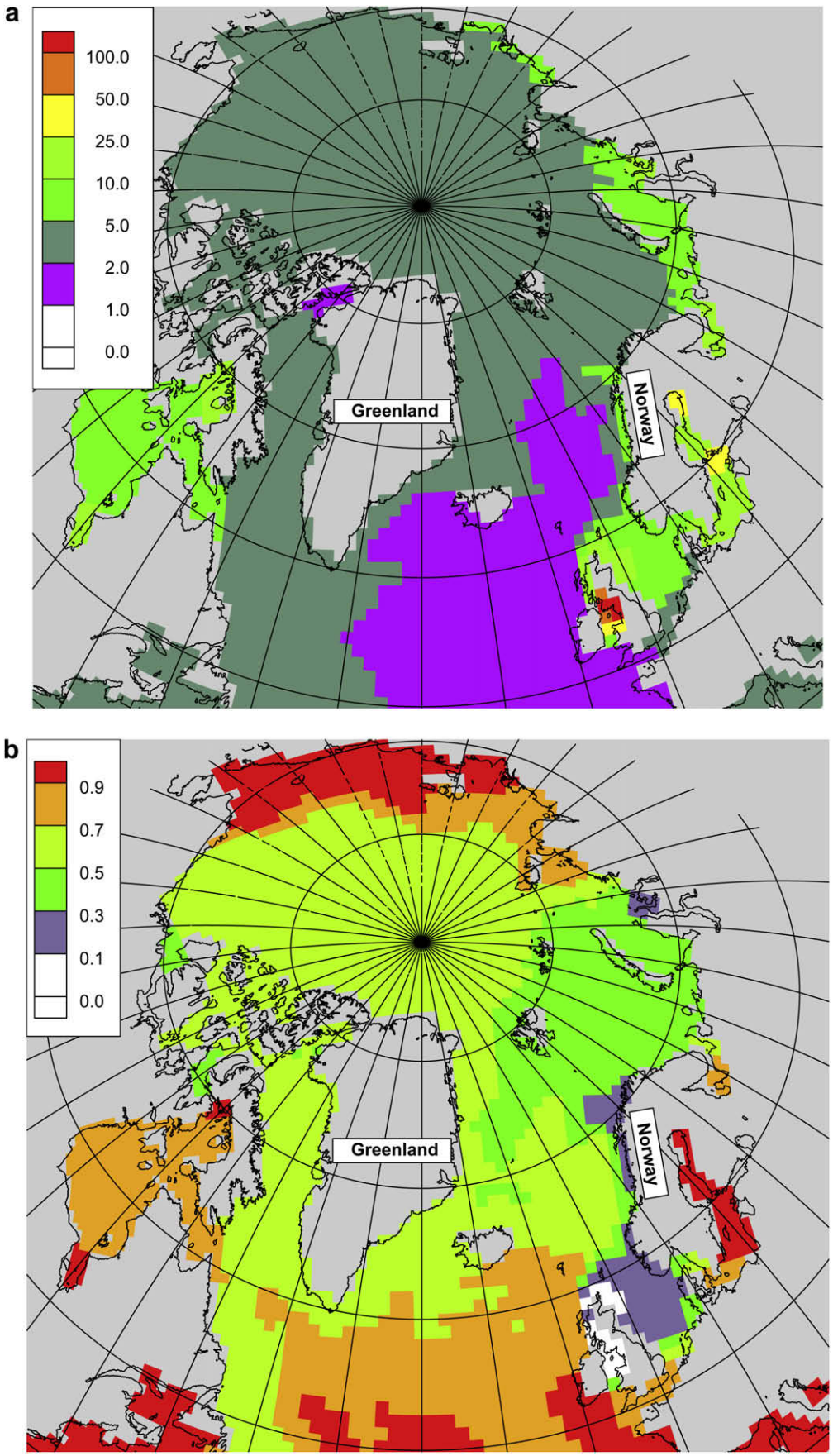

Fig. 6. As Fig. 3, but for year 1980.

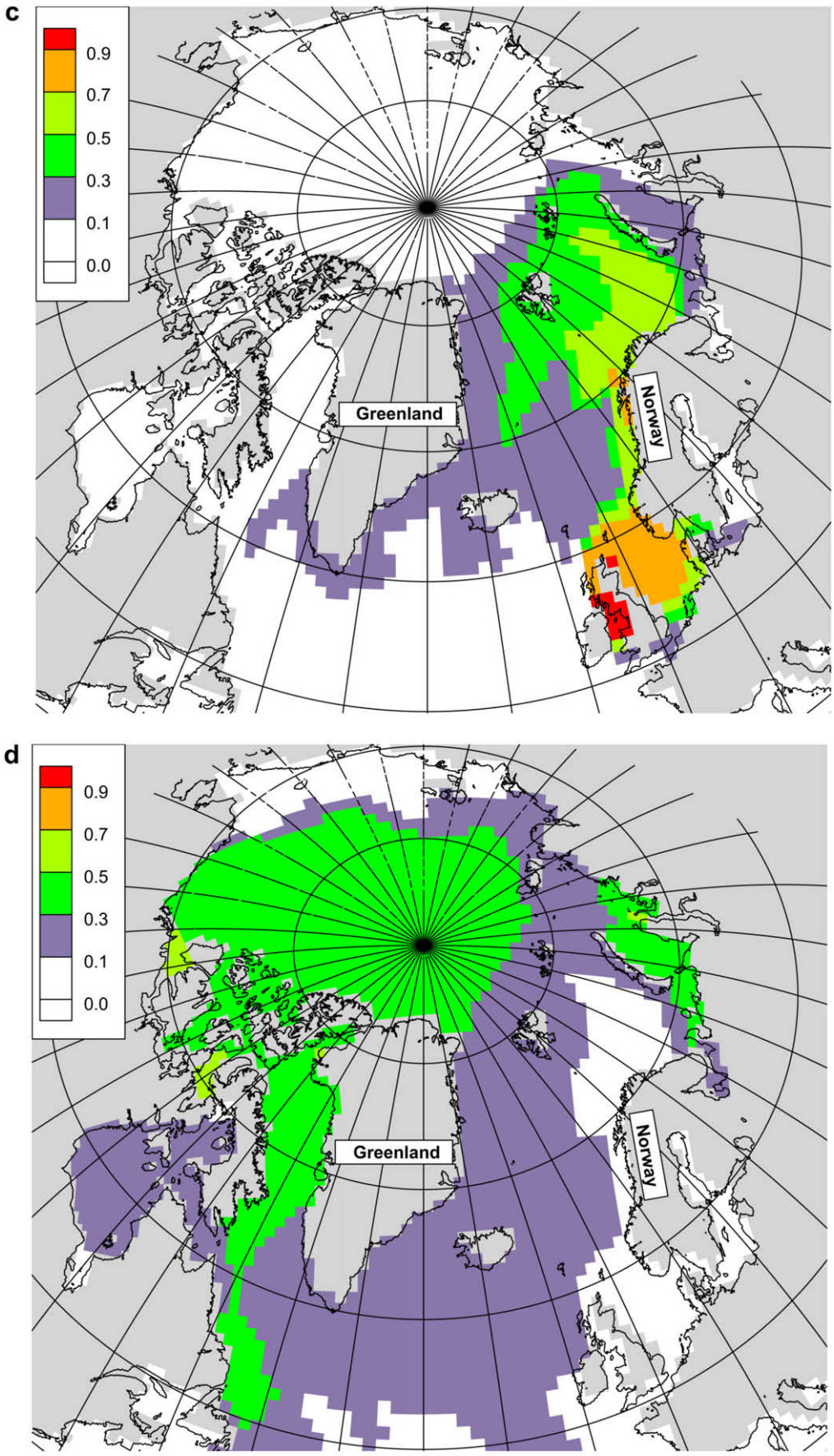

Fig. 6. (*continued*).

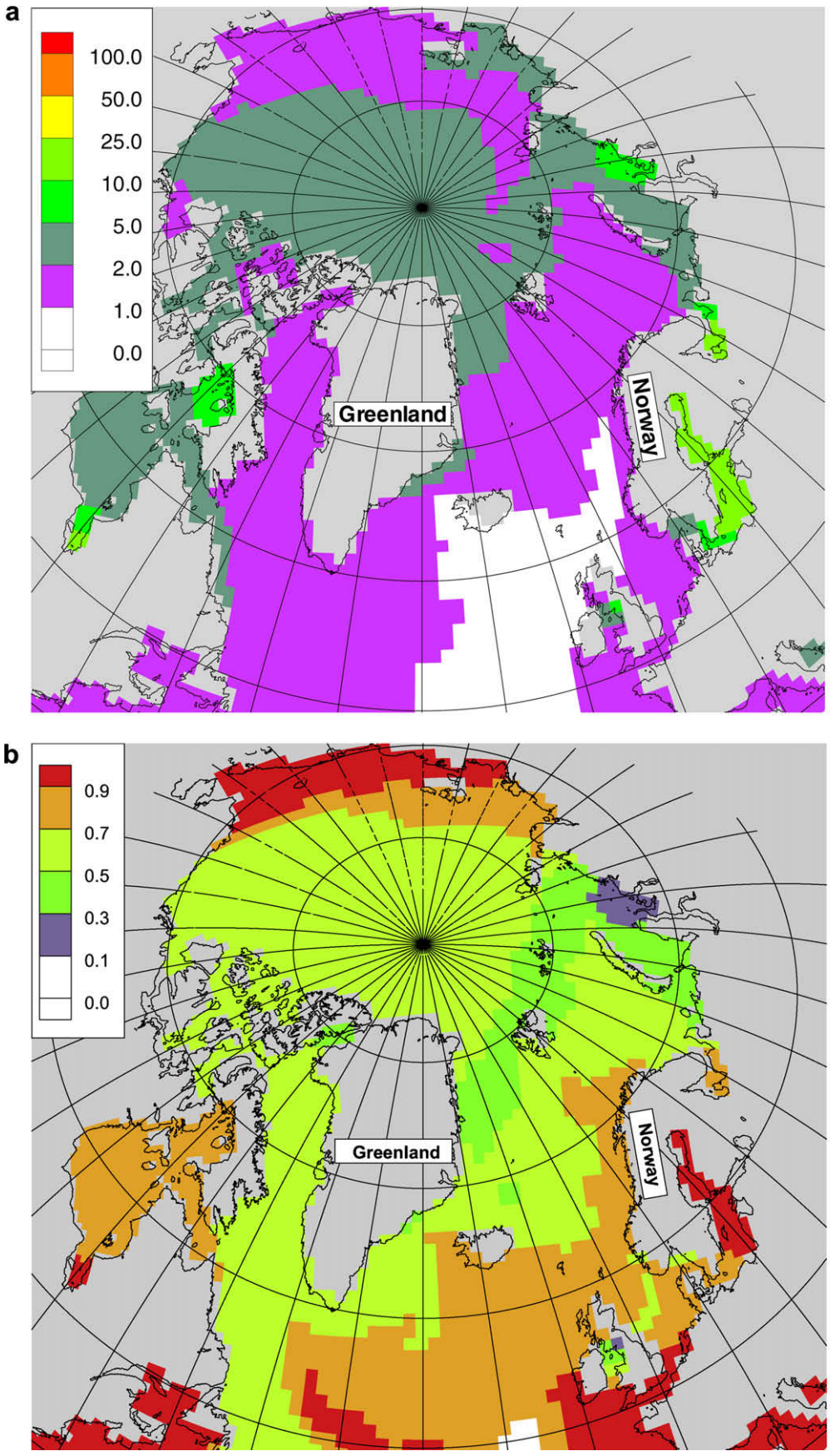

Fig. 7. As Fig. 3, but for year 1990.

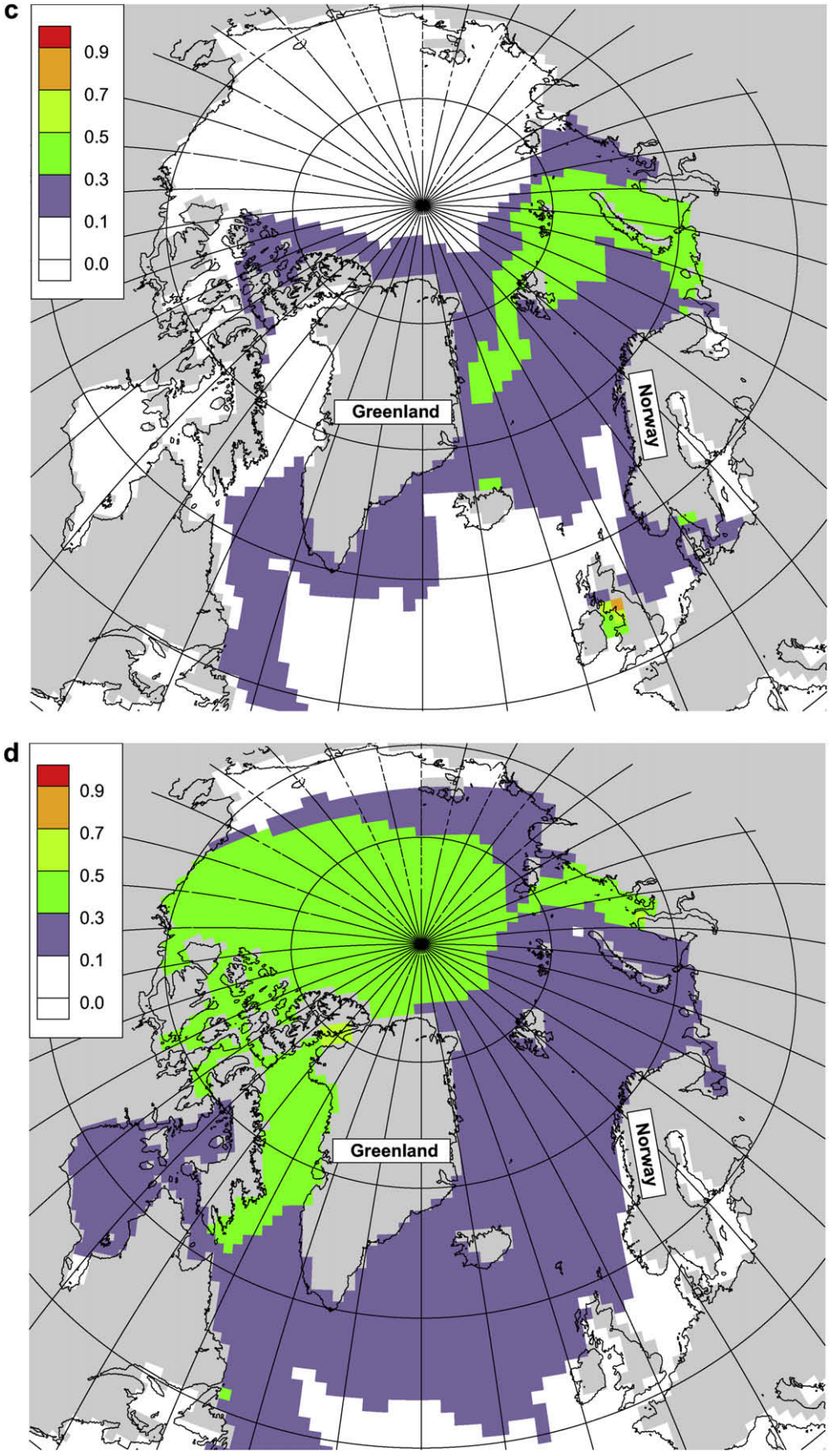

Fig. 7. (*continued*).

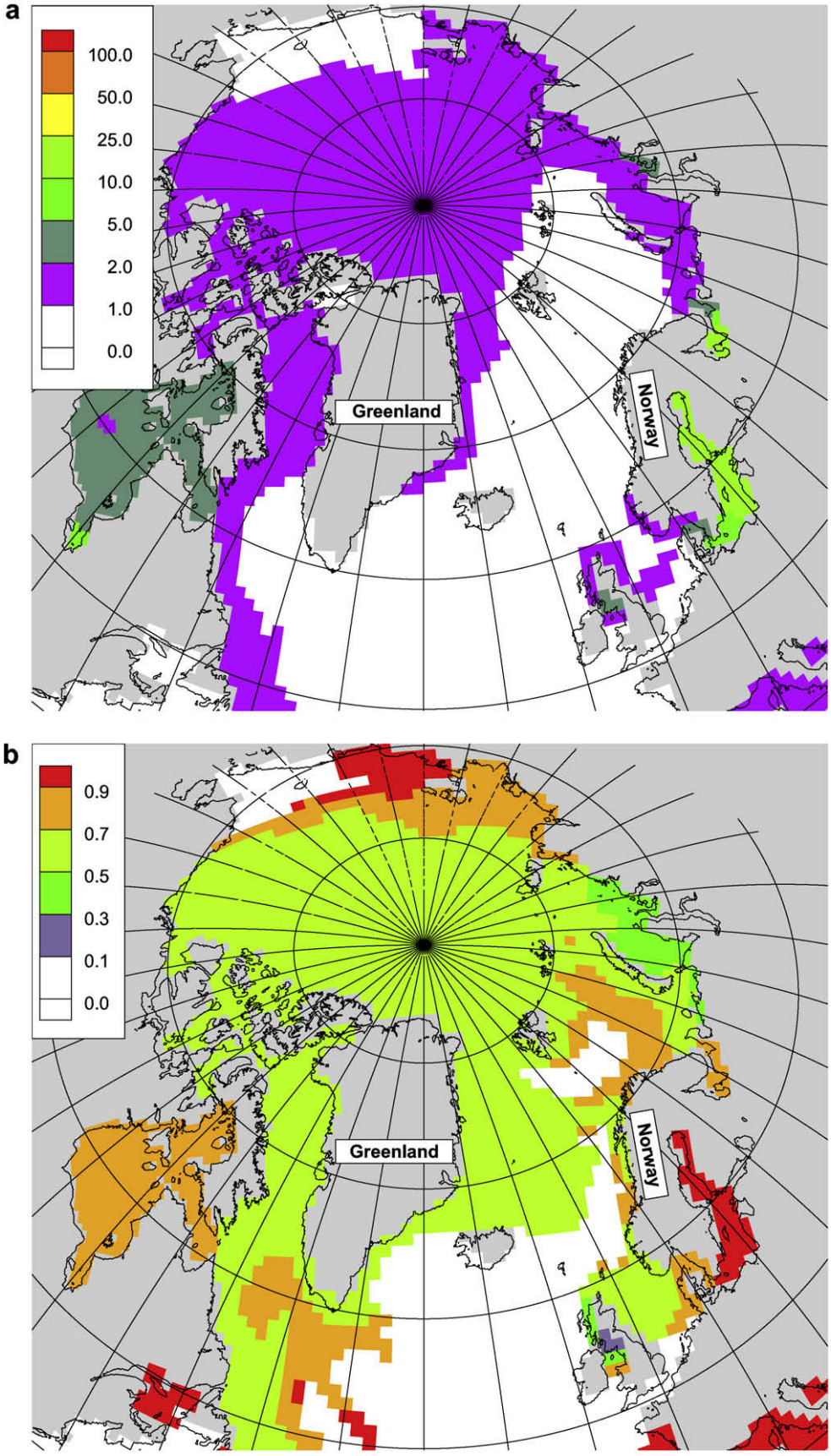

Fig. 8. As Fig. 3, but for year 1999.

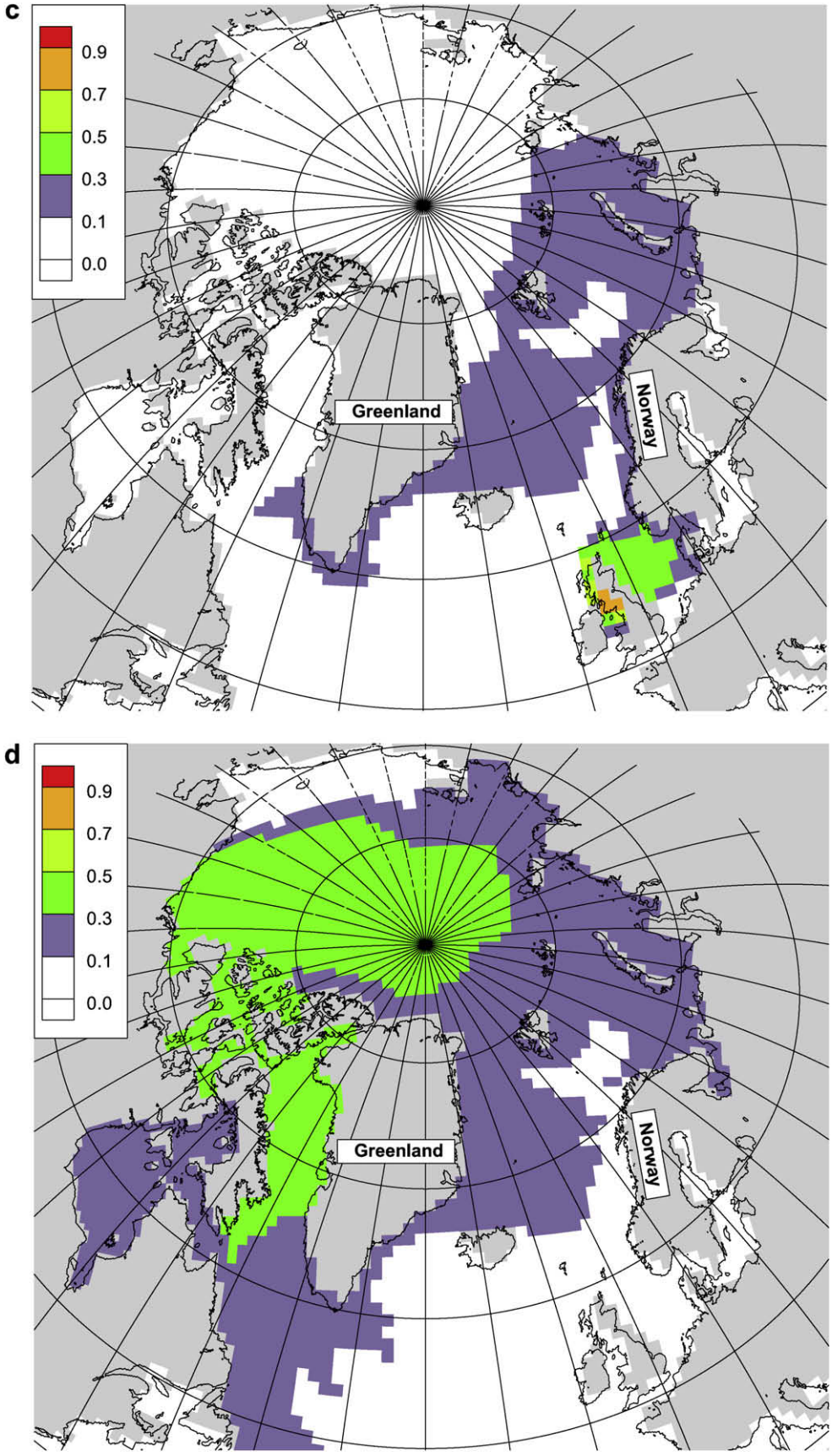

Fig. 8. (*continued*).

river discharge was still a dominant factor in the central Arctic (Fig. 5d). The Sellafield release is mainly confined to the coastal waters of the western Norway (Fig. 5c). During the period between 1970 and 1980, the atmospheric fallout was the dominant source for ^{90}Sr in the central Arctic Ocean, the North Atlantic and the western Nordic Seas (Fig. 6b). Further south, the Sellafield release was responsible for a major part of the ^{90}Sr in the North Sea, along the coast of Norway, and in the southern Barents Sea (Fig. 6c). The Ob river discharge played a less important role in the ^{90}Sr distribution in the central Arctic Ocean (Fig. 6d). In early 1990, the radioactivity of ^{90}Sr was typically lower than 5 Bq m^{-3} in the North Atlantic and the Arctic Ocean (Fig. 7a). The relatively high activity took place in the Kara Sea. The ^{90}Sr distribution in the North Atlantic and the Arctic Ocean was dominant by the atmospheric fallout. The Ob river discharge played a second important role in the ^{90}Sr distribution in the central Arctic Ocean (Fig. 7d). In the Nordic Seas, the distribution of ^{90}Sr was firstly governed by the atmospheric fallout and secondly by the Ob river discharge and the Sellafield release. Towards 1999, the radioactivity was much weaker and the atmospheric fallout dominated over the Ob river discharge and the Sellafield release in both the Arctic Ocean and the Nordic Seas.

The spatial and temporal distributions of ^{90}Sr also indicated the pathways of the spreading from the different sources. The transport of ^{90}Sr from the Sellafield release was similar with the simulated ^{137}Cs (G04) and with the observed estimate (Kershaw and Baxter, 1995). The radionuclide originating from the Ob river spreaded westward towards the Fram Strait, thereafter was branched into two parts with one flowing southward with EGC and the other continuously flowing westward following the northern coast of the Greenland. The Yenisey river discharge was mainly confined to the Kara Sea throughout the integration (figure not shown).

In general, the radioactivity of ^{90}Sr has been drastically declined from 1950 to 1999. The Ob river discharge had strong influence to the Arctic Ocean during 1950s and 1960s. However, the atmospheric fallout is presently the dominant factor in the North Atlantic and Arctic region.

The simulated time evolution of surface ^{90}Sr concentration in the Kara Sea reproduces the observed concentrations in a fairy realistic way (Fig. 9). It follows that the Ob river discharge dominated the ^{90}Sr concentration before 1970 despite the atmospheric fallout induced ^{90}Sr reached its peak value in late 1960s. Between mid-1980 and mid-1990, the atmospheric fallout, the Ob river discharge and the Sellafield release were nearly equal responsible for the surface concentration of ^{90}Sr. It was also evident that the Yenisey river discharge played a minor role in the radioactivity of ^{90}Sr in the Kara Sea region.

6. Spreading of accidentally released ^{90}Sr under present-day and a $2 \times CO_2$ warming scenario

Fig. 10 shows the first 5-yr surface spreading of the accidentally released ^{90}Sr from the Ob river for both the present-day and the $2 \times CO_2$ warming scenario runs. It shows that the ^{90}Sr spreads eastwards following the coast of Siberia and a large amount of accidentally released ^{90}Sr is confined to the Arctic Ocean in the $2 \times CO_2$ warming scenario run, instead of being advected westward towards the Fram Strait under present day climate situation. This finding indicates that the high latitude circulation pattern is quite different between the two forcing situations.

In a similar way, spreading of the accidentally released ^{90}Sr from the Yenisey river (figure not shown) follows that of the Ob discharge: The transport is confined to the Arctic Ocean and the Nordic Seas is radio-waste free in the $2 \times CO_2$ warming scenario run within the first 5 years.

For both the Ob and Yenisey discharges, the maximum surface ^{90}Sr concentrations move out of the Kara Sea in the $2 \times CO_2$ warming scenario run, instead of being blocked in the Kara Sea under the present-day forcing. Consequently, the vulnerable regions for a potential accidental release of ^{90}Sr in the Ob and Yenisey rivers in a future climate is along the coast of the Siberia. The long-term concentration characteristic is provided in Fig. 11. It follows that more of the released ^{90}Sr is confined to the Arctic Ocean in the global warming run, and that the distribution is different in the Arctic Ocean with a change in the location of the ^{90}Sr-enriched waters from the Kara Sea region at the present-day forcing to the coastal, non-European sector in the global warming run. It should be stressed that although large local differences in the spatial distribution of the tracers, the displayed concentration levels are very low.

The reason for the obtained differences in the spatial distributions of the Ob and Yenisey releases of ^{90}Sr follows from Fig. 12. It is clear that the surface circulation in the Artic Ocean features with the clockwise Beaufort Gyre and the Transpolar Drift towards the Fram Strait under present day climate, whereas the clockwise Beaufort Gyre circulation is drastically weakened and the Transpolar Drift disappears under global warming. In fact, the difference between the present-day and the global warming simulations shown in Fig. 12 exceeds the difference between years with high and low NAO forcing at the present-day climate (Fig. 8 in G04).

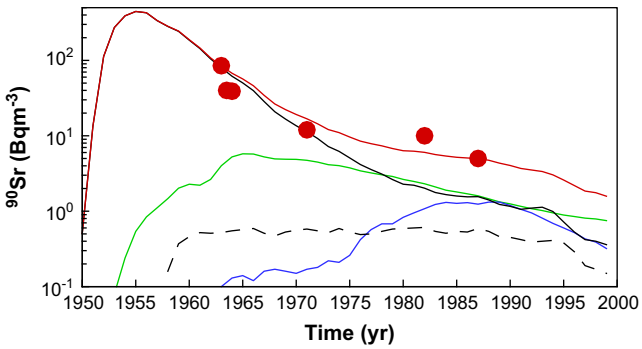

Fig. 9. The temporal evolution of surface concentration of ^{90}Sr (Bq m^{-3}) in the Kara Sea. The red line shows the total ^{90}Sr concentration, the black/green/dashed/blue line denotes the Ob river/the atmospheric fallout/the Yenisey river/the Sellafield discharge induced ^{90}Sr. The filled red circles are observed concentration from Strand et al. (1998). Note the logarithm scale used for the concentrations.

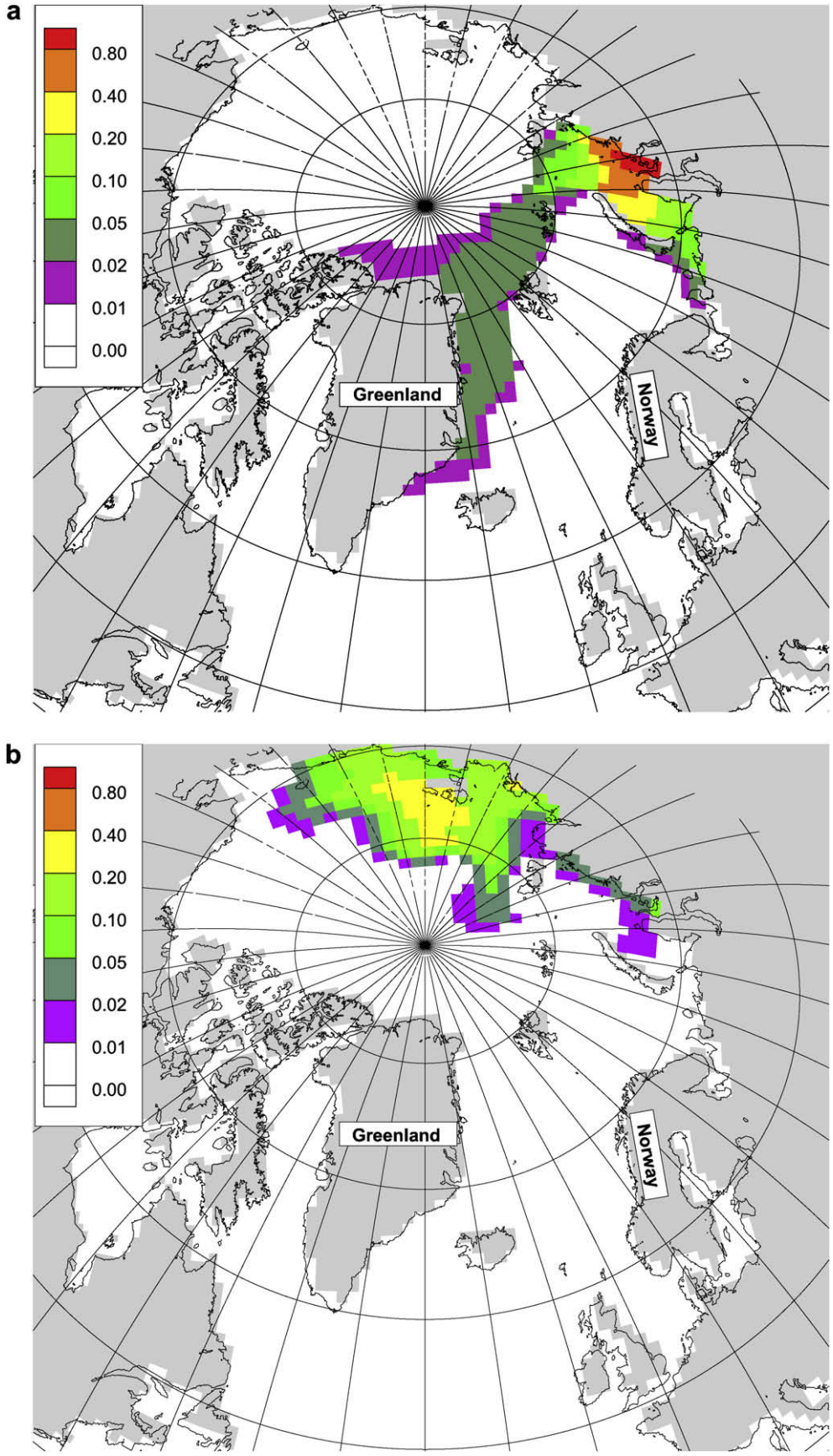

Fig. 10. Spreading of accidental released ^{90}Sr (Bq m^{-3}) from Ob river at yr 5 under present climate condition (left panel) and under the global warming scenario (double CO_2; right panel).

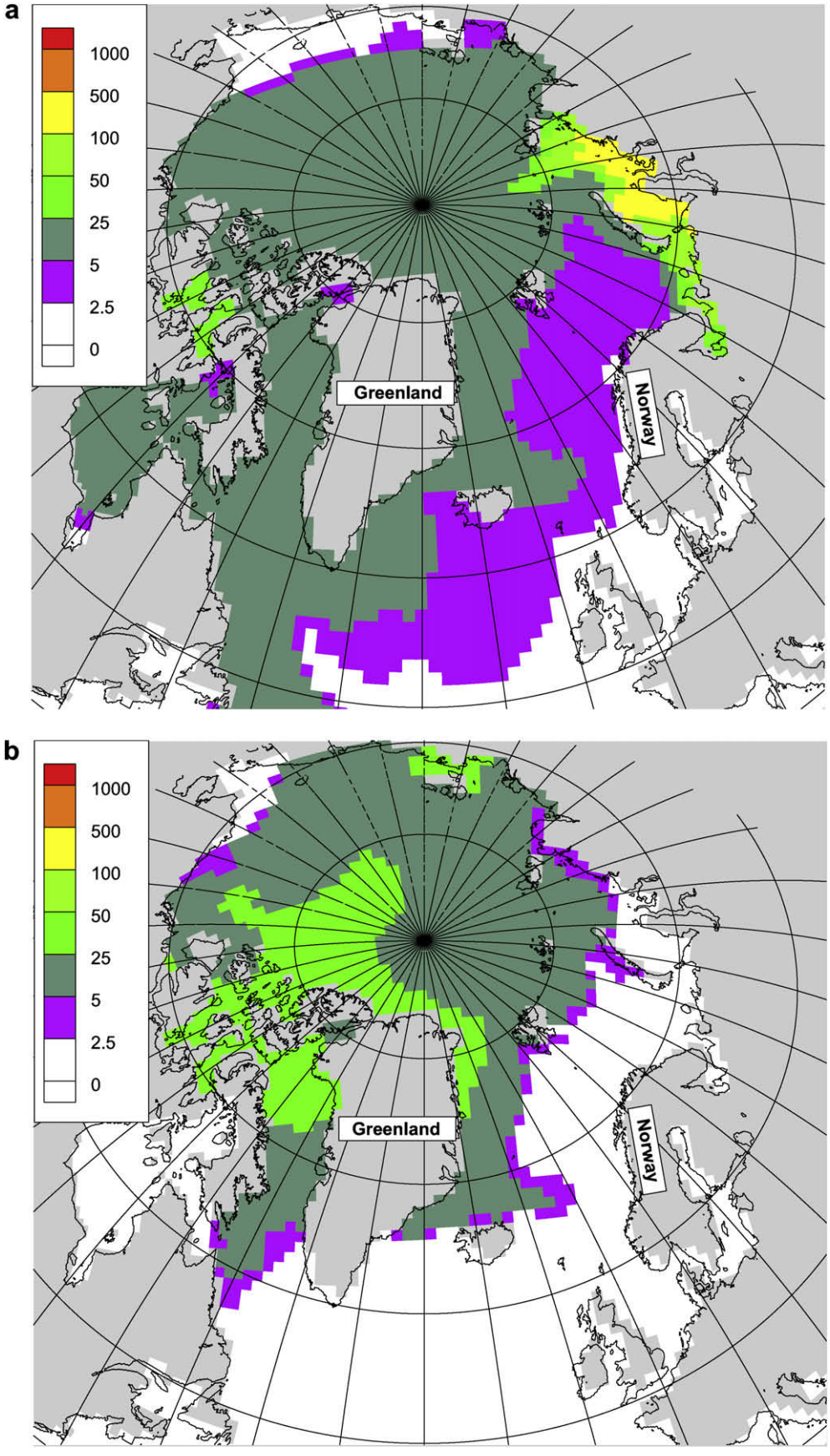

Fig. 11. As Fig. 10, but for yr 20. Note the unit for the contour is 10^{-4} Bq m^{-3}.

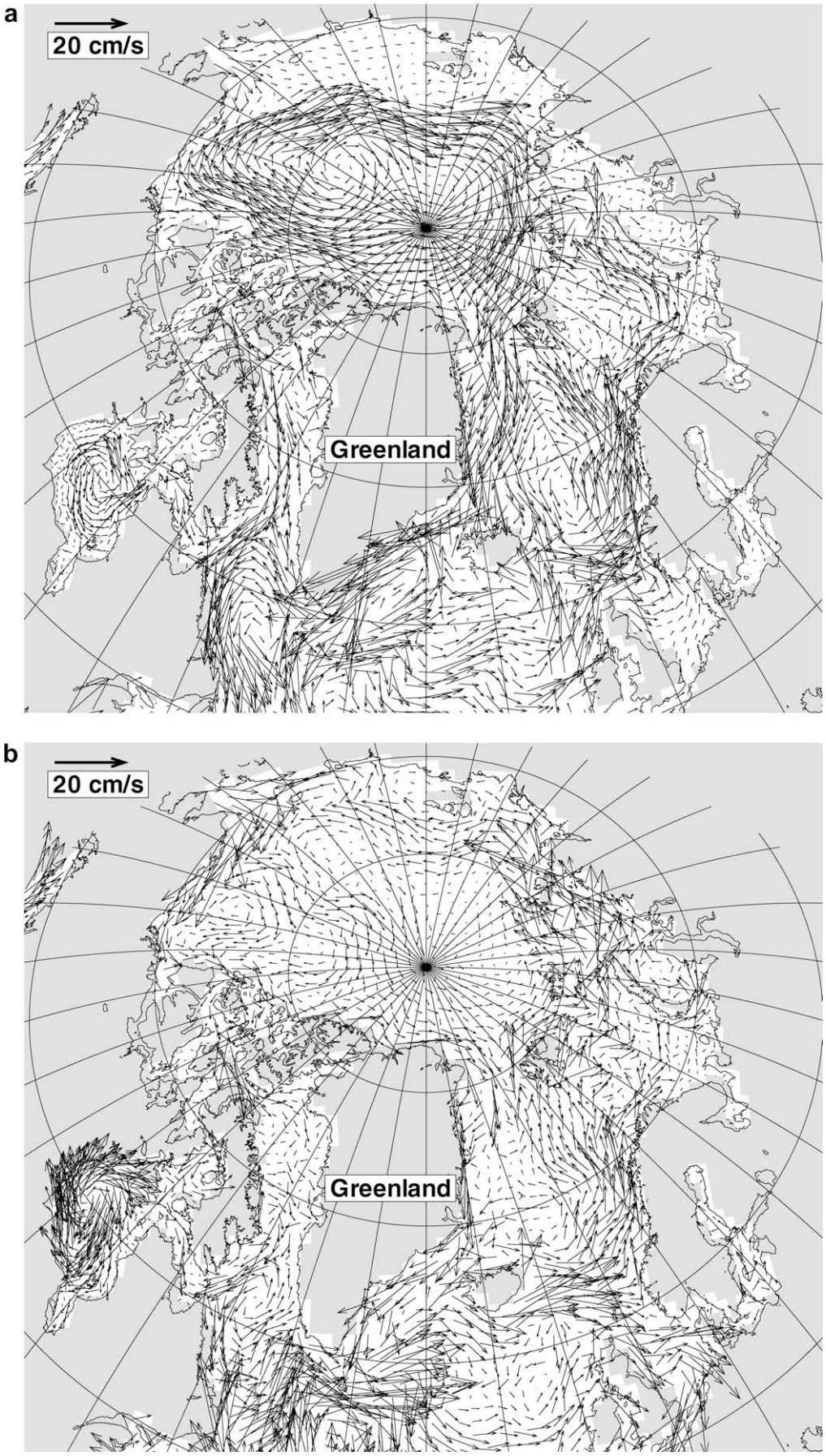

Fig. 12. The simulated surface circulation between 1970 and 2000 (a), between 2050 and 2080 under the global warming scenario (b) and the difference (present-day minus global warming) between the two periods (c).

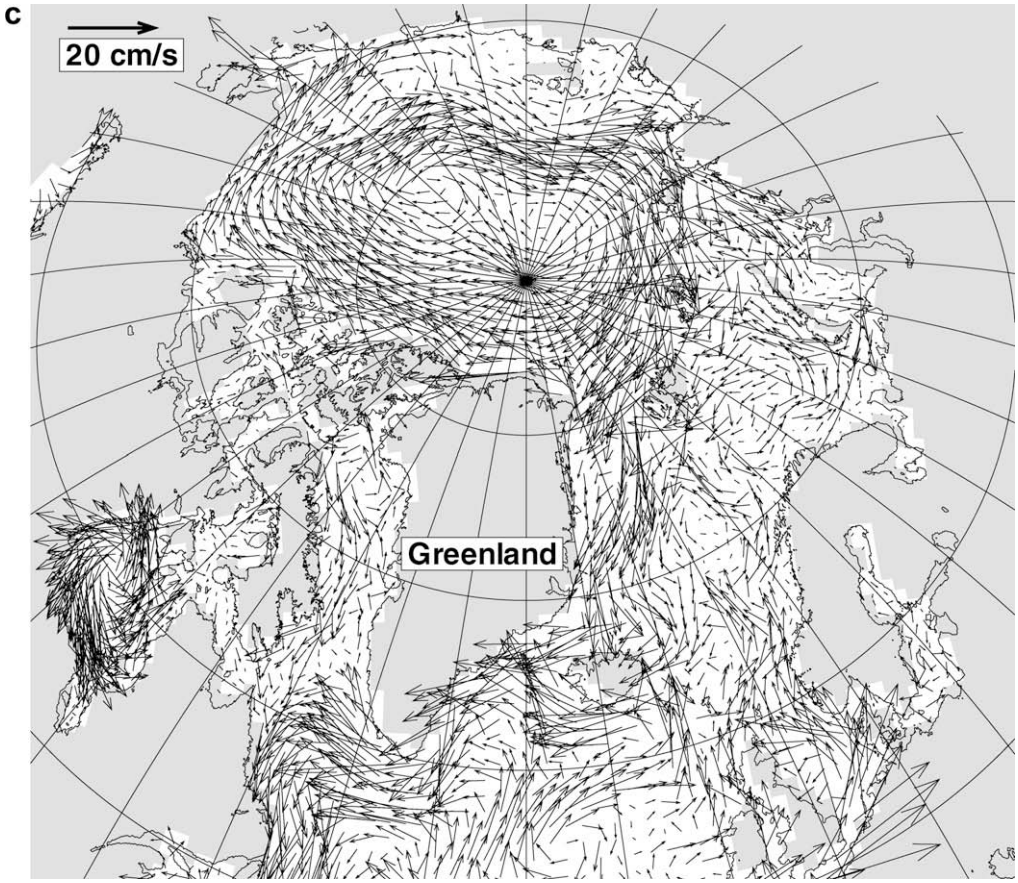

Fig. 12. (*continued*).

7. Discussion and conclusion

A synoptic-forced, global version of MICOM has been used to examine the transport of the conservative radionuclide ^{90}Sr originating from the nuclear bomb testing, the Sellafield release and the Ob and Yenisey river discharges. The relative importance of the different sources on the spatial–temporal distributions of the surface ^{90}Sr over the period of 1948–1999 is assessed. Furthermore, the spreading of the potential accident release of ^{90}Sr from the Ob and Yenisey rivers has been simulated under the present-day climate and for the first time under the global warming scenario ($2 \times CO_2$).

The overall radioactivity of ^{90}Sr has been reduced from 1950 to 1999. However, it is interesting to note that the Ob river discharge was dominant in the Arctic Ocean and in the coastal waters following the eastern and south-eastern coast of Greenland from 1950s to 1960s, whereas the atmospheric fallout was dominant in the North Atlantic Ocean and off coast of western Norway during the same period. The Sellafield release was dominant off the coast of the western Norway in the 1980s. For the late 1990s, the atmospheric fallout was the main contributor for the radioactivity of ^{90}Sr in the North Atlantic and the Arctic Ocean.

As a passive tracer in sea water, the transport of ^{90}Sr is determined by the ocean circulation and the mixing. The simulated pathway of the Sellafield release to the Arctic Ocean is fairly realistic (also see G04). For the applied source functions of Ob and Yenisey river discharges, the spreading of the Ob river discharge was branched into two parts with one part circulating in the Arctic Ocean and the other flowing southward with the EGC, whereas the Yenisey river discharge was mainly confined to the Kara Sea over the simulated period of 1948–1999.

Without sufficient observation, it is impossible to judge whether the spreading of the radionuclide from the various sources is realistic in the Arctic Ocean. For instance, Nies et al. (1998) found that the peak values of the Sellafield release induced ^{137}Cs were obtained in 1985 and 1990 at the North Pole using a regional model forced by the climatological fields, whereas the peak values were mainly found on the Atlantic side of the Pole (G04). However, it is well known that the sea-ice drift and the surface water circulation in the Arctic Ocean are closely associated with the natural variability modes of the atmospheric circulation, namely NAO and AO (Arctic Oscillation; Thompson and Wallace, 1998). Therefore, it is important to use realistic atmospheric forcing fields to simulate the transport of the tracers in the Arctic Ocean (G04).

It is shown that the simulated time evolutions of ^{137}Cs are in fairly good agreement with the observations in the coastal waters of eastern Scotland, west of Norway, and in the Barents Sea (G04). Furthermore, the simulated time evolution of the surface ^{90}Sr in the Kara Sea matches the observed concentrations quite well (Fig. 9). It follows that the Ob river discharge dominated the ^{90}Sr concentration before 1970 despite the atmospheric fallout induced ^{90}Sr reached its peak value in the late 1960s. Between mid-1980 and mid-1990, the atmospheric fallout, the Ob river discharge and the Sellafield release are equally important for the ^{90}Sr surface concentration. It is also evident that the Yenisey river discharge played a minor role in the distribution of ^{90}Sr concentration in the Kara Sea region.

It is also worth mentioning that for the ^{90}Sr in the Arctic Ocean, the Ob river discharge highly dominated in the 1950s and 1960s (Figs. 3 and 4), that the Ob river was equally important with the atmospheric fallout in the 1970s (Fig. 5), and that the atmospheric

fallout was more dominant from 1980 to 1999 (Figs. 6–8). In the Arctic, the contribution from the Sellafield ^{90}Sr release is very small throughout the integration (Figs. 3–8).

The difference between the present-day and the $2 \times CO_2$ warming scenario runs for the accidental releases of ^{90}Sr in the Ob and Yenisey rivers is illustrated in Figs. 10 and 11. The results indicate that more of the released ^{90}Sr is confined to the Arctic Ocean in the global warming run, particularly in the near coastal, non-European part of the Arctic Ocean. It shows that a global warming scenario may change the surface circulation more than the changes between persistent low and high NAO forcing in the region.

It should be emphasized that the spreading under the global warming scenario is highly dependent on the applied 21st century forcing, and by that hypothetical. Nevertheless, the proposed and performed twin experiments are a powerful – and consistent – method to assess future spreading of radionuclides for specific release scenarios. For more reliable prediction, the ensemble and multi-model simulations should be performed.

Acknowledgements

This study is supported by the EU-project Simulation Scenarios for Potential Radioactive Spreading in the 21 Century from Rivers and External Sources in the Russian Arctic Coastal Zone (RADARC; ICA2-CT-2000-10037) and supported by the Norwegian Research Council founded project Arctic Radioactive Contaminations (ARC). The authors are grateful to Dr. Sven Nielsen for providing time histories of the radionuclides and to Bergen Climate Model (BCM) group for the surface forcing fields under the global warming scenario, in particular, for the help from Ingo Bethke. The model development has been supported by the Research Council of Norway through the RegClim project, KlimaProg's "Spissfors-kningsmidler", and the Programme of Supercomputing.

References

Bentsen, M., Evensen, G., Drange, H., Jenkins, A.D., 1999. Coordinate transformation on a sphere using conformal mapping. Mon. Wea. Rev. 127, 2733–2740.

Bleck, R., Rooth, C., Hu, D., Smith, L.T., 1992. Salinity-driven thermohaline transients in a wind- and thermohaline-forced isopycnic coordinate model of the North Atlantic. J. Phys. Oceanogr. 22, 1486–1515.

Drange, H., Gerdes, R., Gao, Y., Karcher, M., Kauker, F., Bentsen, M., 2005. Ocean general circulation modelling of the Nordic Seas. In: Drange, H., Dokken, T., Furevik, T., Berger, W., Gerdes, R. (Eds.), The Nordic Seas: An Integrated Perspective. AGU Monograph, vol. 158. American Geophys. Union., Washington, DC, pp. 199–220.

Eldevik, T., Straneo, F., Sando, A., Furevik, T., 2005. Pathways and export of Greenland sea water. In: Drange, H., Dokken, T., Furevik, T., Gerdes, R., Berger, W. (Eds.), The Nordic Seas: An Integrated Perspective. Geophysical Monograph, vol. 158. American Geophysical Union, Washington, DC, pp. 89–104.

Furevik, T., Bentsen, M., Drange, H., Kindem, I., Kvamstø, N., Sorteberg, A., 2003. Description and validation of the Bergen Climate Model: ARPEGE coupled with MICOM. Clim. Dyn. 21, 27–51. doi:10.1007/s00382-003-0317-5.

Gao, Y., Drange, H., Bentsen, M., 2003. Effects of diapycnal and isopycnal mixing on the ventilation of CFCs in the North Atlantic in an isopycnic coordinate OGCM. Tellus 55B (3), 837–854.

Gao, Y., Drange, H., Bentsen, M., Johannessen, O.M., 2004. Simulating transport of non-Chernobyl ^{137}Cs and ^{90}Sr in the North Atlantic–Arctic region. J. Environ. Radioact. 71 (1), 1–16. doi:10.1016/S0265-931X(03)00108-5.

Gao, Y., Drange, H., Bentsen, M., Johannessen, O.M., 2005. Tracer-derived transit time of the waters in the eastern Nordic Seas. Tellus 57B, 332–340.

Gerland, S., Lind, B., Dowdall, M., Karcher, M., Kolstad, A.K., 2003. ^{99}Tc in seawater in the West Spitsbergen Current and adjacent areas. J. Environ. Radioact. 69 (1–2), 119–127.

Hansen, B., Østerhus, S., 2000. North Atlantic–Nordic Seas exchanges. Prog. Oceanogr. 45 (2), 109–208.

Hatun, H., Sando, A., Drange, H., Hansen, B., Valdimarsson, H., 2005. Influence of the Atlantic subpolar gyre on the thermohaline circulation. Science 309, 1841–1844.

Hurrell, W., 1995. Decadal trends in the north Atlantic oscillation: regional temperatures and precipitation. Science 269, 676–679.

Ingvaldsen, R., Loeng, H., Asplin, L., 2002. Variability in the Atlantic inflow to the Barents Sea based on a one-year time series from moored current meters. Continental Shelf Res. 22, 505–519.

Johannessen, O., Dziuba, N., Koshebutsky, K., Maderich, V., Zheleznyak, M., 2003. The final scientific report for simulation scenarios for potential radioactive spreading in the 21 century from rivers and external sources in the Russian Arctic Coast Zone. Tech. rep., Nansen Environmental and Remote Sensing Center, Bergen, Norway.

Kalnay, E., Kanamitsu, M., Kistler, R., Collins, W., Deaven, D., co authors, 1996. The NCEP/NCAR 40-year reanalysis project. Bull. Am. Meteorol. Soc. 77 (3), 437–471.

Karcher, M.J., Gerland, S., Harms, I.H., Iosjpe, M., Heldal, H.E., Kershaw, P.J., Sickel, M., 2004. The dispersion of ^{99}Tc in the Nordic Seas and the Arctic Ocean: a comparison of model results and observations. J. Environ. Radioact. 74, 185–198.

Kershaw, P., Baxter, A., 1995. The transfer of reprocessing wastes from north-west Europe to the Arctic. Deep Sea Res. 42, 1413–1448.

Levitus, S., Boyer, T.P., 1994. World Ocean Atlas 1994 Volume 4: Temperature. NOAA Atlas NESDIS 4, Washington, D.C., USA.

Levitus, S., Burgett, R., Boyer, T.P., 1994. World Ocean Atlas 1994 Volume 3: Salinity. NOAA Atlas NESDIS 3, Washington, D.C., USA.

Margvelashvili, N., Maderich, V., Zheleznyak, M., 1997. THREETOX-computer code to simulate three-dimensional dispersion of radionuclides in homogeneous and stratified water bodies. Radiat. Prot. Dosimetry 73, 177–180.

Nies, H., Harms, H., Karcher, M., Dethleff, D., Bahe, C., Kuhlmann, G., Oberhuber, J., Backhaus, J., Kleine, E., Loewe, P., Matishov, D., Stepanov, A., Vasiliev, O., 1998. Anthropogenic radioactivity in the Nordic Seas and the Arctic Ocean – results of a joint project. Dtsch. Hydrogr. Z. 50 (4), 313–343.

Nilsen, J.E.Ø, Gao, Y., Drange, H., Furevik, T., Bentsen, M., 2003. Simulated North Atlantic–Nordic Seas water mass exchanges in an isopycnic coordinate OGCM. Geophys. Res. Lett. 30 (10), 1536. doi:10.1029/2002GL016597.

Orre, S., Gao, Y., Drange, H., Nilsen, J., 2007. A reassessment of the dispersion properties of 99Tc in the North and Norwegian Sea. J. Marine Syst. 68 (1–2), 24–38, doi:10.1016/j.jmarsys.2006.10.009.

Sorteberg, A., Furevik, T., Drange, H., Kvamsto, N., 2005. Effects of simulated natural variability on Arctic temperature projections. Geophys. Res. Lett. 32, L18708. doi:10.1029/2005GL023404.

Strand, P., Aarkrog, A., Bewers, J., Tsaturov, Z., Magnusson, S., 1996. Radioactive contamination of the Arctic marine environment. In: Radionuclides in the Oceans – Inputs and Inventories. Inst. de Protection et de Surete Nucleaire, France, pp. 95–119.

Strand, P., Balonov, M., Aarkrog, A., Bewers, M.J., Howard, B., Salo, A., Tsaturov, Y.S., 1998. Radioactivity. In: AMAP (Ed.), AMAP Assessment Report: Arctic Pollution Issues. Arctic Monitoring and Assessment Programme (AMAP), Oslo, Norway, p. 859.

Strand, P., Howard, B., Aarkrog, A., Balonov, M., Tsaturov, Y., Bewers, J., Salo, A., Sickel, M., Bergman, R., Rissanen, K., 2002. Radioactive contamination in the Arctic–sources, dose assessment and potential risks. J. Environ. Radioact. 60, 5–21.

Thompson, D., Wallace, J., 1998. The arctic oscillation signature in the wintertime geopotential height and temperature fields. Geophys. Res. Lett. 25, 1297–1300.

Tsumune, D., Aoyama, M., Hirose, K., 2003. Numerical simulation of ^{137}Cs and ^{239,240}Pu concentration by an ocean general circulation model. J. Environ. Radioact. 69, 61–84.

Zheleznyak, M., Demchenko, R., Khursin, S., Kuzmenko, Y., Tkalich, P., Vitjuk, N., 1992. Mathematical modelling of radionuclide dispersion in the Pripyat–Dnieper aquatic system after the Chernobyl accident. Sci. Tot. Environ. 112, 89–114.